



MSC 78A45

BOUNDARY INTEGRAL EQUATIONS AND ITS NUMERICAL ANALYSIS IN DIFFRACTION OF TE MODE ON SLITS IN THE IMPEDANCE PLANE

Y.V. Gandel, K.V. Nesvit

Karazin Kharkiv National University,

Svobody Sq. 4, Kharkiv, 61022, Ukraine, e-mail: yuriy.gandel@gmail.com, nesvit.k@gmail.com

Abstract. It is described the integral equations (IEs) approach to building the discrete mathematical model of the diffraction problem of TE wave on slits in the impedance plane. These IEs are connected with the boundary-value problem of stationary wave equation. Such a type of problems leads to systems of the boundary IEs with logarithmic singularities in kernels which are solved by an efficient discrete singularities method (DSM). It is demonstrated that discrete mathematical models of the wave diffraction problem on slits and subsequent numerical experiment are efficient way for solving the problem under consideration. It is performed the extensive numerical analysis of the TE mode diffraction on slits and it has shown some main characteristics of electromagnetic fields at different values of parameters. Numerical results cover radiation and diffraction patterns of the scattered fields from different orders of pre-Cantor grating, and the electric and magnetic components of scattered electromagnetic fields in the near zone for various impedances of gratings: Ag, Cu, Al, Mg, Ni and constantan.

Keywords: diffraction problem, boundary integral equations, numerical analysis, discrete singularities method.

1. Introduction

the numerical analysis of the TE mode diffraction on slits in the impedance plane is described in the paper. The overall aim of the work is to perform numerical experiments based on the developed discrete mathematical model of boundary integral equations with help of the efficient discrete singularities method.

Reduction of boundary-value problems connected with the stationary wave equation to integral equations arise in the problem of diffraction on plane-parallel structures from the theory of electromagnetic waves.

Main publications in this area are [1] (in Russian) and [2] where boundary value problems in diffraction theory are solved by mathematical methods which reduce them to boundary singular and hypersingular IEs.

One of classical problems which open wide opportunities for application to calculation of antennas, open resonators and other microwave devices, is the scattering of electromagnetic waves by a thin strip. The pioneer work representing the application of DSM to solve a scattering problem of plane wave by superconducting strips was introduced in [3]. For more complex problems with DSM applications see [4], [5], [6].

The model which is under consideration in this paper, is the approximation of real fractal antenna [7] in 2D. Fractal antennas are used in a variety of modern mobile devices



due to their compact size and broadband properties which have made them essential in wireless communication, Bluetooth, Wi-Fi and GSM standards. Their theoretical research is important, both in terms of developing mathematical tools for solving complicated boundary value problems of electrodynamics, and a more accurate approximation to real physical models. Therefore, numerical analysis of diffraction problems of TE modes by slits in a Cantor set on the $[-1, 1]$ interval in the impedance plane is a challenging task and an actual problem.

We have calculated total and scattered fields, diffraction and radiation patterns as functions of metal properties, orders of pre-Cantor gratings, angles and frequencies of incident TE waves. Analysis of diffraction patterns is important as they describe main characteristics and features of diffraction phenomenon in the problem under consideration. This paper highlights the performance and efficiency of the developed numerical DSM.

2. Formulation of the diffraction problem of TE mode

To solve a 2D diffraction problem we calculate the total field which satisfies Maxwell's equations:

$$\begin{aligned} \operatorname{rot} \bar{E}(y, z) - i\omega\mu \bar{H}(y, z) &= 0, \\ \operatorname{rot} \bar{H}(y, z) + i\omega\mu \bar{E}(y, z) &= 0, \\ \operatorname{div} \bar{E}(y, z) &= 0, \quad \operatorname{div} \bar{H}(y, z) = 0; \end{aligned} \quad (1)$$

supplemented with Shchukin-Leontovich's impedance boundary condition:

$$[\bar{n}, \bar{E}] = -Z_c [\bar{n}, [\bar{n}, \bar{H}]], \quad (2)$$

where $Z_c = \frac{1+i}{\sqrt{2}} \sqrt{\frac{\omega\mu_c}{\sigma_c}}$ is the resistivity of metal and \bar{n} is a unitary surface normal vector to the impedance plane. Besides, the total field must also satisfy the Sommerfeld radiation conditions and the Meixner edges condition.

We consider the case of the E-polarization: $(E_x, 0, 0)$, $(0, H_y, H_z)$. Propagation direction of plane wave is given by direction of the wave vector \bar{k} (Fig. 2).

The only non-zero component of electric field satisfy all the aforementioned conditions and also the two-dimensional Helmholtz equation without of metallic strips:

$$\frac{\partial^2 E_x}{\partial y^2} + \frac{\partial^2 E_x}{\partial z^2} + \varepsilon\mu\omega^2 E_x = 0, \quad \varepsilon\mu\omega^2 = k^2. \quad (3)$$

The non-zero magnetic field components are expressed by Maxwell's equations (1):

$$H_y = \frac{1}{i\omega\mu} \frac{\partial E_x}{\partial z}, \quad H_z = -\frac{1}{i\omega\mu} \frac{\partial E_x}{\partial y}. \quad (4)$$

Cartesian coordinate system is chosen so that the set of slits is located in the XY plane and the X axis is parallel to the strips' edges.

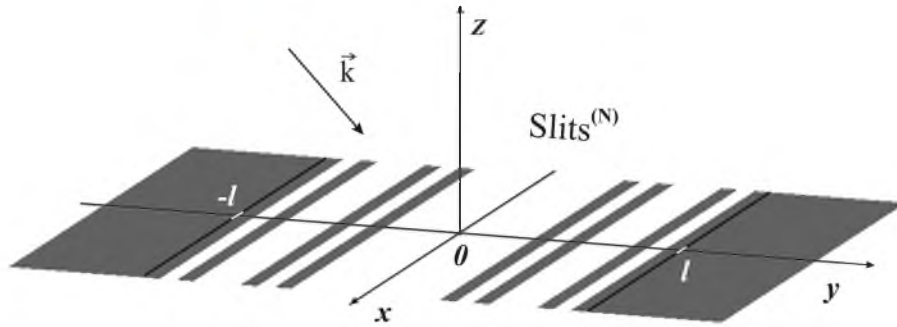


Fig. 1. Schematic of the considered diffraction structure.

$$\text{Slits}^{(N)} = \left\{ (x, y, z) \in \mathbb{R}^3 : x \in \mathbb{R}, y \in \text{Sl}_l^{(N)}, z = 0 \right\}, \quad \text{Sl}_l^{(N)} = \bigcup_{q=1}^{2^N-1} (a_q^N, b_q^N).$$

It is convenient to switch to dimensionless coordinates:

$$\varsigma = \frac{x}{l}, \quad \xi = \frac{y}{l}, \quad \zeta = \frac{z}{l}, \quad \alpha_q^N = \frac{a_q^N}{l}, \quad \beta_q^N = \frac{b_q^N}{l}, \quad \kappa = kl, \quad \text{Sl}^{(N)} = \bigcup_{q=1}^{2^N-1} (\alpha_q^N, \beta_q^N).$$

The E-polarized plane wave falls from infinity at the angle α :

$$u_{inc}^N(\xi, \zeta) = E_\varsigma(\xi, \zeta) = e^{i\kappa(\xi \sin \alpha - \zeta \cos \alpha)}, \tag{5}$$

Here, α is the angle between the positive direction of the axis ξ and the propagation direction of a plane monochromatic wave, and κ is the absolute value of wave vector (see Fig. 2).

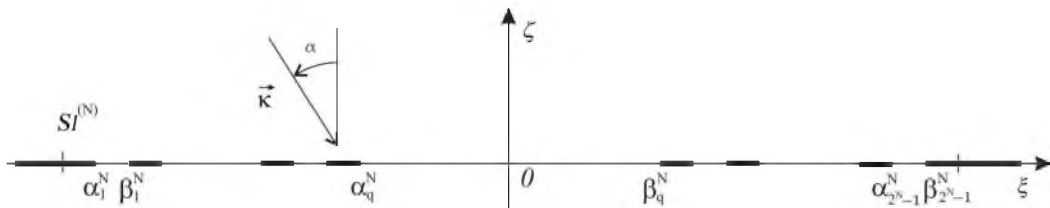


Fig. 2. Cross-section of the diffraction structure in the $\xi\zeta$ plane.

The total field is considered to have the form:

$$u^{(N)}(\xi, \zeta) = \begin{cases} u_0^N(\xi, \zeta) + u_+^N(\xi, \zeta), & \xi > 0, \\ u_-^N(\xi, \zeta), & \xi < 0, \end{cases} \tag{6}$$

where $u_0^N(\xi, \zeta)$ is a known solution to the Helmholtz equation. It represents the sum of incident and reflected waves in the half-space $\zeta \geq 0$ when slits are closed. The functions $u_+^N(\xi, \zeta)$, $u_-^N(\xi, \zeta)$ are considered as Fourier series in the integral form:



$$u_+^N(\xi, \zeta) = \int_{-\infty}^{+\infty} C_+^N(\lambda) e^{i\lambda\xi - \gamma(\lambda)\zeta} d\lambda, \quad \xi > 0, \quad (7)$$

$$u_-^N(\xi, \zeta) = \int_{-\infty}^{+\infty} C_-^N(\lambda) e^{i\lambda\xi + \gamma(\lambda)\zeta} d\lambda, \quad \xi < 0. \quad (8)$$

These series satisfy the Helmholtz equation (3), the boundary conditions which follow from (2), the Sommerfeld and Meixner conditions, and the conditions of conjugation in the slits. The radiation condition will be satisfied if $\gamma(\lambda)$ is given by $\text{Re } \gamma(\lambda) \geq 0$, $\text{Im } \gamma(\lambda) \leq 0$.

3. Boundary Integral Equations

As shown in the monograph [1] and the paper [3] the boundary-value problem (1) considering all mentioned conditions is reduced to two systems of coupled integral equations:

$$\left\{ \begin{array}{l} \int_{-\infty}^{+\infty} [C_+^N(\lambda) - C_-^N(\lambda)] (\gamma(\lambda) + A) e^{i\lambda\xi} d\lambda = 0, \quad \xi \in \mathbb{C} \setminus \text{SI}^{(N)}, \\ \int_{-\infty}^{+\infty} [C_+^N(\lambda) - C_-^N(\lambda)] e^{i\lambda\xi} d\lambda = -u_0^N(\xi, +0), \quad \xi \in \text{SI}^{(N)}, \end{array} \right. \quad (9)$$

$$\left\{ \begin{array}{l} \int_{-\infty}^{+\infty} [C_+^N(\lambda) + C_-^N(\lambda)] (\gamma(\lambda) + A) e^{i\lambda\xi} d\lambda = 0, \quad \xi \in \mathbb{C} \setminus \text{SI}^{(N)}, \\ \int_{-\infty}^{+\infty} [C_+^N(\lambda) + C_-^N(\lambda)] \gamma(\lambda) e^{i\lambda\xi} d\lambda = \frac{\partial u_0^N}{\partial \zeta}(\xi, +0), \quad \xi \in \text{SI}^{(N)}, \end{array} \right. \quad (10)$$

where $A = i\kappa \frac{Z_0}{Z_e}$ determines the impedance of material, $Z_0 = \sqrt{\frac{\mu_0}{\varepsilon_0}}$ is the free space impedance, and μ_0, ε_0 are magnetic and dielectric constants.

Let us introduce two new unknown functions:

$$\Lambda_+^N(\eta) = - \int_{-\infty}^{+\infty} [C_+^N(\lambda) - C_-^N(\lambda)] (\gamma(\lambda) + A) e^{i\lambda\eta} d\lambda, \quad \eta \in \mathbb{R}, \quad (11)$$

$$\Lambda_-^N(\eta) = - \int_{-\infty}^{+\infty} [C_+^N(\lambda) + C_-^N(\lambda)] (\gamma(\lambda) + A) e^{i\lambda\eta} d\lambda, \quad \eta \in \mathbb{R}. \quad (12)$$

From coupled equations (9), (10) we obtain properties of the functions (11), (12):



$$\Lambda_+^N(\xi) = 0, \quad \Lambda_-^N(\xi) = 0, \quad \xi \in \mathbb{C}S\mathbb{I}^{(N)}.$$

Therefore by applying inverse Fourier transform on functions $\Lambda_+^N(\eta)$, $\Lambda_-^N(\eta)$ we have the following relation between the unknown coefficients:

$$C_+^N(\lambda) - C_-^N(\lambda) = -\frac{1}{2\pi(\gamma(\lambda) + A)} \int_{S\mathbb{I}^N} \Lambda_+^N(\eta) e^{-i\lambda\eta} d\eta, \tag{13}$$

$$C_+^N(\lambda) + C_-^N(\lambda) = -\frac{1}{2\pi(\gamma(\lambda) + A)} \int_{S\mathbb{I}^N} \Lambda_-^N(\eta) e^{-i\lambda\eta} d\eta. \tag{14}$$

As shown in [8] the coupled equations (9), (10) are reduced to boundary integral equations of the 1st and 2nd kinds with logarithmic singularities in kernels:

$$\frac{1}{\pi} \int_{S\mathbb{I}^N} \ln |\xi - \eta| \Lambda_+^N(\eta) d\eta + \frac{1}{\pi} \int_{S\mathbb{I}^N} K_{11}^N(\eta, \xi) \Lambda_+^N(\eta) d\eta = f_1^N(\xi), \quad \xi \in S\mathbb{I}^N, \tag{15}$$

$$\Lambda_-^N(\xi) + \frac{A}{\pi} \int_{S\mathbb{I}^N} \ln |\xi - \eta| \Lambda_-^N(\eta) d\eta + \frac{A}{\pi} \int_{S\mathbb{I}^N} K_{11}^N(\eta, \xi) \Lambda_-^N(\eta) d\eta = f_2^N(\xi), \quad \xi \in S\mathbb{I}^N,$$

where $K_{11}^N(\eta, \xi)$, $f_1^N(\xi)$, $f_2^N(\xi)$ are smooth known functions.

To reduce the equation (15) on $S\mathbb{I}^N$ to equations on a set of intervals $S\mathbb{I}_q^N = (\alpha_q^N, \beta_q^N)$, $q = \overline{1, 2^N - 1}$, we introduce restrictive conditions to functions:

$$\Lambda_+^N(\eta)|_{\eta \in S\mathbb{I}_q^N} = \Lambda_{+,q}^N(\eta), \quad \Lambda_-^N(\eta)|_{\eta \in S\mathbb{I}_q^N} = \Lambda_{-,q}^N(\eta), \quad \Lambda_-^N(\xi)|_{\xi \in S\mathbb{I}_p^N} = \Lambda_{-,p}^N(\xi), \tag{16}$$

$$f_1^N(\xi)|_{\xi \in S\mathbb{I}_p^N} = f_{1,p}^N(\xi), \quad f_2^N(\xi)|_{\xi \in S\mathbb{I}_p^N} = f_{2,p}^N(\xi).$$

The Meixner condition will be satisfied if the unknown functions (11), (12) are represented in the form:

$$\Lambda_{+,q}^N(\eta) = \frac{v_{+,q}^N(\eta)}{\sqrt{(\beta_q^N - \eta)(\eta - \alpha_q^N)}}, \quad \Lambda_{-,q}^N(\eta) = \frac{v_{-,q}^N(\eta)}{\sqrt{(\beta_q^N - \eta)(\eta - \alpha_q^N)}}, \tag{17}$$

$$\Lambda_{-,p}^N(\xi) = \frac{v_{-,p}^N(\xi)}{\sqrt{(\beta_p^N - \xi)(\xi - \alpha_p^N)}}, \quad \xi \in S\mathbb{I}_p^N, \quad \eta \in S\mathbb{I}_p^N.$$

By choosing a normalized interval (-1,1) the variables transform accordingly:



$$g_q^{(N)} : (-1, 1) \rightarrow (\alpha_q^N, \beta_q^N) : t \rightarrow g_q^{(N)}(t) = \frac{\beta_q^N - \alpha_q^N}{2}t + \frac{\beta_q^N + \alpha_q^N}{2},$$

$$\eta = g_q^{(N)}(t), \quad \xi = g_q^{(N)}(t_0), \quad |t| < 1, \quad |t_0| < 1, \quad \eta \in \text{Sl}_q^N, \quad \xi \in \text{Sl}_p^N, \quad q = \overline{1, 2^N - 1}. \quad (18)$$

Considering (16)-(18) and excluding logarithmic singularity at $p = q$ from equations (9)-(10), we obtain a system of boundary integral equations of the 1st and 2nd kind with logarithmic singularities on a normalized interval for $p = \overline{1, 2^N - 1}$:

$$\left\{ \begin{array}{l} \frac{1}{\pi} \int_{-1}^1 \ln |t - t_0| v_{+,p}^N(g_p^{(N)}(t)) \frac{dt}{\sqrt{1-t^2}} + \\ + \frac{1}{\pi} \sum_{q=1}^{2^N-1} \int_{-1}^1 M_{1,qp}^N((g_q^{(N)}(t)), (g_p^{(N)}(t_0))) v_{+,q}^N(g_q^{(N)}(t)) \frac{dt}{\sqrt{1-t^2}} = f_{1,p}^N(g_p^{(N)}(t_0)), \\ \\ \frac{2v_{-,p}^N(g_p^{(N)}(t_0))}{(\beta_p^N - \alpha_p^N) \sqrt{1-t_0^2}} + \frac{A}{\pi} \int_{-1}^1 \ln |t - t_0| v_{-,p}^N(g_p^{(N)}(t)) \frac{dt}{\sqrt{1-t^2}} + \\ + \frac{A}{\pi} \sum_{q=1}^{2^N-1} \int_{-1}^1 M_{1,qp}^N((g_q^{(N)}(t)), (g_p^{(N)}(t_0))) v_{-,q}^N(g_q^{(N)}(t)) \frac{dt}{\sqrt{1-t^2}} = f_{2,p}^N(g_p^{(N)}(t_0)), \end{array} \right. \quad (19)$$

where $M_{i,qp}^N((g_q^{(N)}(t)), (g_p^{(N)}(t_0)))$, $f_{i,p}^N(g_p^{(N)}(t_0))$, $i = 1, 2$, are smooth known functions.

4. Discrete Mathematical Model

Discrete mathematical model has been developed with the help of an efficient numerical method DSM [1]. The unknown functions

$$v_{+,q}^N(g_q^N(t)), \quad v_{-,q}^N(g_q^N(t)),$$

and smooth ones

$$M_{i,qp}^N((g_q^{(N)}(t)), (g_p^{(N)}(t_0))), \quad f_{i,p}^N(g_p^{(N)}(t_0)), \quad i = 1, 2,$$

are interpolated by a Lagrange polynomial of $(n - 1)$ -th degree in the nodes which are the nulls of Chebyshev's polynomials of the 1st kind:

$$t_k^n = \cos\left(\frac{2k-1}{2n}\pi\right), \quad k = \overline{1, n}.$$



From the mathematical model in (19) we have obtained the system of approximate solutions. At the next step, using the quadrature formulas [9] for integrals with logarithmic singularity and integrals of the smooth functions, we derive the system of the linear algebraic equations (SLAE) for the values of unknown functions in the node points:

$$v_{+,q}^{N,(n-1)}(g_q^N(t_k^n)), \quad v_{-,q}^{N,(n-1)}(g_q^N(t_k^n)).$$

At collocated points we chose another set of Chebychev's nodes:

$$t_j^n = \cos\left(\frac{2j-1}{2n}\pi\right), \quad j = \overline{1, n}.$$

Therefore, we have obtained a SLAE for $p = \overline{1, 2^N - 1}, \quad j = \overline{1, n}$:

$$\left\{ \begin{aligned} & -\frac{1}{n} \sum_{k=1}^n v_{+,p}^{N,(n-1)}(g_p^N(t_k^n)) \left[\ln 2 + 2 \sum_{r=1}^{n-1} T_r(t_j^n) \frac{T_n(t_k^n)}{r} \right] + \\ & + \frac{1}{n} \sum_{q=1}^{2^N-1} \sum_{k=1}^n M_{1,qp}^N(g_q^N(t_k^n), g_p^N(t_j^n)) v_{+,q}^{N,(n-1)}(g_q^N(t_k^n)) = f_{1,p}^{N,(n-1)}(t_j^n), \\ & \frac{2 \sum_{k=1}^n v_{-,p}^{N,(n-1)}(g_p^N(t_k^n)) l_{n-1,k}^I(t_j^n)}{(\beta_p^N - \alpha_p^N) \sqrt{1 - (t_j^n)^2}} \\ & - \frac{A}{n} \sum_{k=1}^n v_{-,p}^{N,(n-1)}(g_p^N(t_k^n)) \left[\ln 2 + 2 \sum_{r=1}^{n-1} T_r(t_j^n) \frac{T_n(t_k^n)}{r} \right] + \\ & + \frac{1}{n} \sum_{q=1}^{2^N-1} \sum_{k=1}^n M_{2,qp}^N(g_q^N(t_k^n), g_p^N(t_j^n)) v_{-,q}^{N,(n-1)}(g_q^N(t_k^n)) = f_{2,p}^{N,(n-1)}(t_j^n), \end{aligned} \right. \quad (20)$$

where $M_{i,qp}^N((g_q^N(t_k^n)), (g_p^N(t_j^n)))$, $f_{i,p}^N(g_p^N(t_j^n))$, $i = 1, 2$ are smooth known functions.

By solving this SLAE we find the values of unknown functions in the node points and calculate the coefficients (13), (14) for the total and scattered fields (7), (8).

Using the asymptotic representation of Hankel's functions, and (6), (7):

$$u_+^N(r, \varphi) \sim \int_{-\kappa}^{\kappa} C_+^N(\lambda) e^{ir(\lambda \cos \varphi + \sqrt{\kappa^2 - \lambda^2} \sin \varphi)} d\lambda, \quad u_-^N(r, \varphi) \sim \int_{-\kappa}^{\kappa} C_-^N(\lambda) e^{ir(\lambda \cos \varphi - \sqrt{\kappa^2 - \lambda^2} \sin \varphi)} d\lambda,$$

$$H_0^{(1)}(\kappa r) \sim \sqrt{\frac{2}{\pi \kappa r}} e^{i(\kappa r - \frac{\pi}{4})}, \quad r = \sqrt{\xi^2 - \zeta^2},$$



we derive the expressions for the far field radiation patterns of the scattered and diffracted fields:

$$D_{\pm}^N(\varphi) = \lim_{r \rightarrow \infty} \frac{u_{\pm}^N(r, \varphi)}{\sqrt{\frac{2}{\pi \kappa r}} e^{i(\kappa r - \frac{\pi}{4})}}. \quad (21)$$

Using results of [1], [8], [11] we can estimate the rate of convergence of approximate solutions to the exact metric in Hilbert's space, and the uniform metric for physical quantities.

Using these formulas for radiation patterns, unknown coefficients and also the total, scattered and diffracted fields, we have performed the extensive numerical analysis of the TE mode diffraction problem.

5. Numerical Results

Figs. 3 and 4 shows the total and scattered E-fields as functions of different metals: argentum (Ag), cuprum (Cu), aluminum (Al), magnesium (Mg), nickel (Ni). It can be concluded that with Ni strips the largest amplitude of electric field is observed; the Ag and Cu strips show similar results and have the lowest E-field amplitudes.

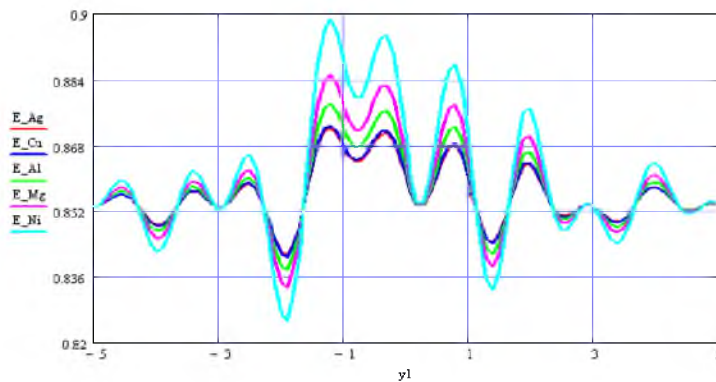


Fig. 3. Near field of the total field for different metals, where $N = 3$, $\alpha = 20^\circ$, $l = 0.02m$, $f = 11.2GHz$.

Fig. 5 shows radiation patterns (RPs) of E-field as functions of orders of pre-Cantor gratings. The left one shows the RP (not normalized) and demonstrates the change in length of the antenna lobe. The normalized RP is shown on the right and demonstrates visible changes in the shape of antenna lobes. It can be concluded that the amount of lobes and their length grow with the gratings order N .

Fig. 6 shows the near field of the scattered field for the absolute value of magnetic components.

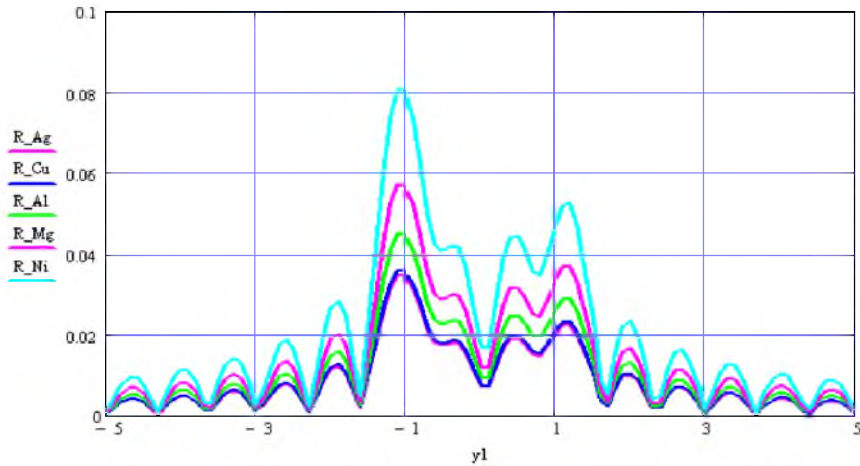


Fig. 4. Near field of the scattered field for different metals, where $N = 3$, $\alpha = 20^0$, $l = 0.02m$, $f = 11.2GHz$.

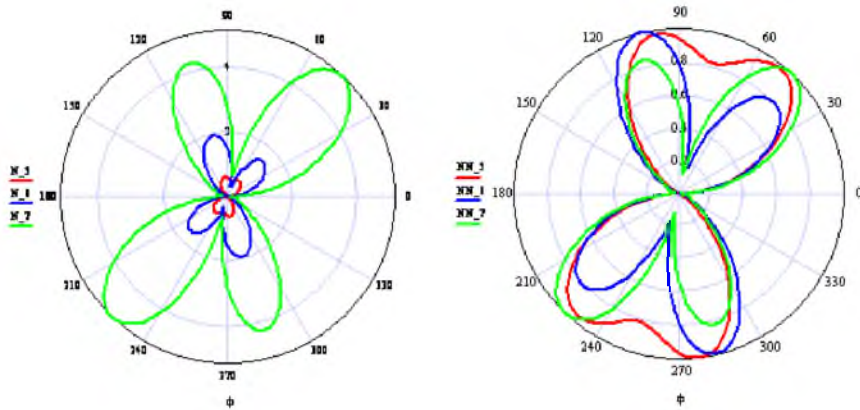


Fig. 5. Far field radiation patterns for Mg and various orders of gratings: $N = 4, 5, 6$, where $\alpha = 20^0$, $l = 0.01m$, $f = 15GHz$.

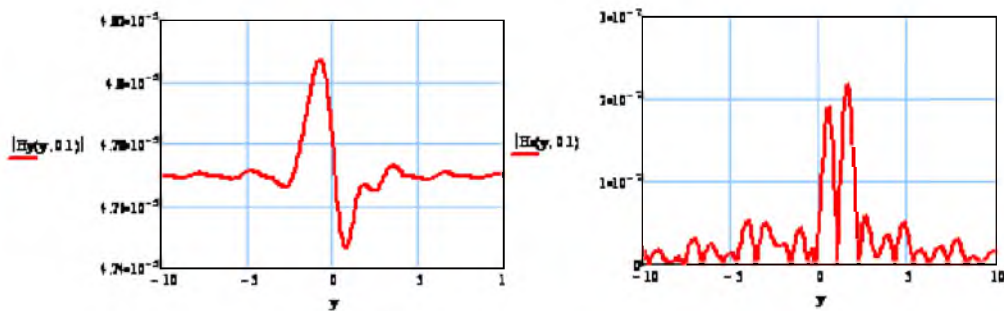


Fig. 6. Near field of the scattered field for the absolute value of magnetic components for Cu, where $\alpha = 20^0$, $l = 0.01m$, $f = 15GHz$.



Fig. 7 shows the near field diffraction patterns (DPs) of scattered fields depending on the order of pre-Cantor gratings: $N = 2, 3, 4$.

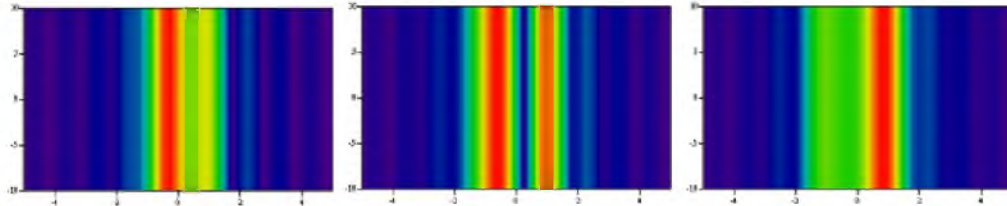


Fig. 7. Near field diffraction patterns of scattered field for various orders of gratings $N = 2, 3, 4$ for Cu, where $\alpha = 20^\circ$, $l = 0.01m$, $f = 15GHz$.

Figs. 8 and 9 show the near field of the total and scattered fields, and near field DPs for the strips from constantan where 0° and 20° are angles of incident TE wave. The main attractive feature of constantan alloy is its resistivity which is constant over a wide range of temperatures.

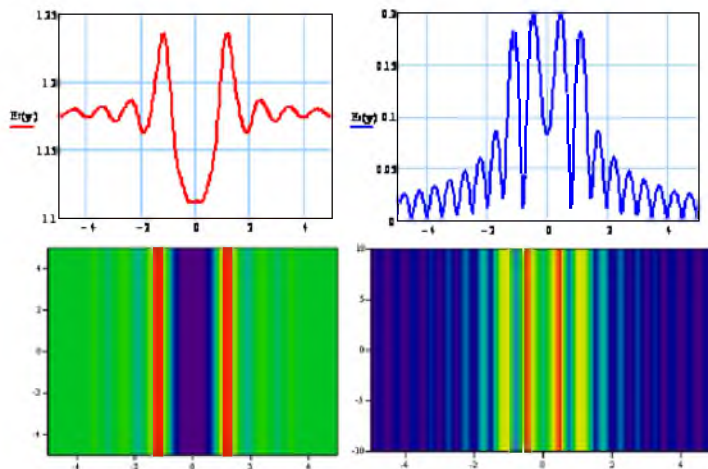


Fig. 8. Near field of the total and scattered E-field and its diffraction patterns for constantan, where $N = 3$, $\alpha = 0^\circ$, $l = 0.01m$, $f = 30GHz$.

Fig. 10 shows the near field RPs for different frequencies: 15GHz and 30GHz. It can be seen that the amount of lobes grows with the increase of frequency.

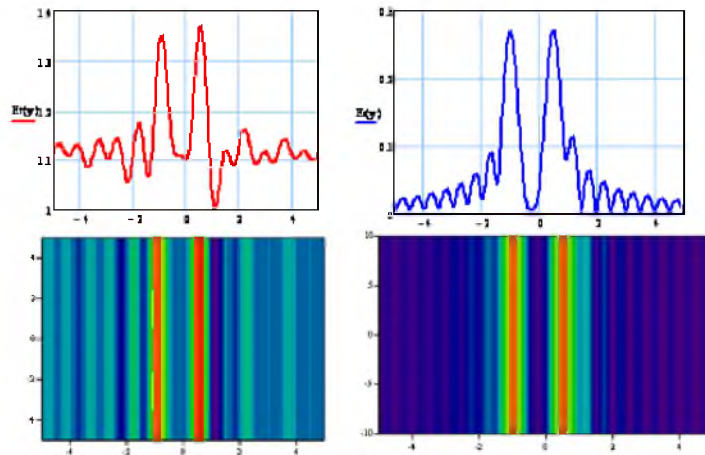


Fig. 9. Near field of the total and scattered E-field and its diffraction patterns for constantan, where $N = 3$, $\alpha = 20^0$, $l = 0.01m$, $f = 30GHz$.

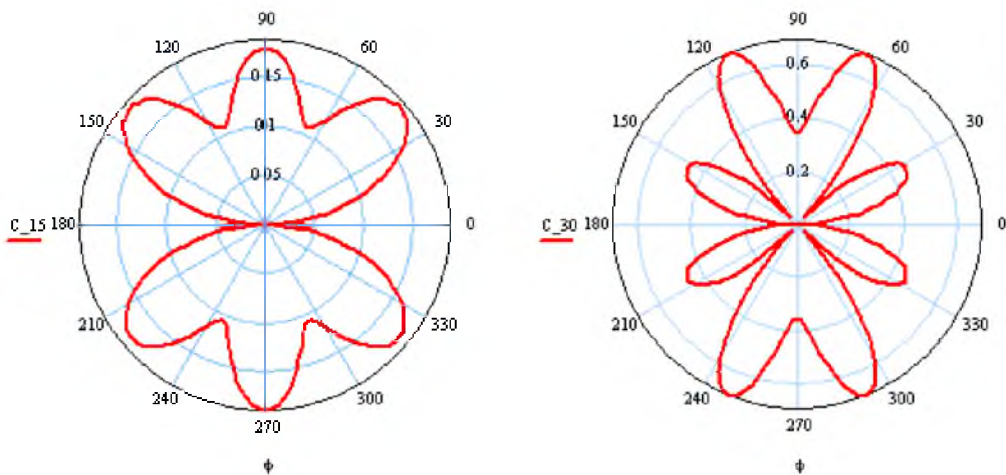


Fig. 10. Far field radiation patterns for constantan, where $N = 3$, $\alpha = 0^0$, $l = 0.01m$, $f = 15GHz$ and $f = 30GHz$.

6. Conclusions

The goal of this work was to perform numerical analysis of the diffraction problem of TE mode on slits in the impedance plane using DSM and to improve the approach of solving such problems with discrete numerical methods. Handling this problem with the mathematical theory of diffraction is a complicated task due to the involved integrals with logarithmic singularities in the kernels. This has raised an objective for us to develop a discrete mathematical model which would resolve these difficulties. We have successfully solved the boundary IEs with the help of a numerical DSM and special quadrature formulas with the nodes in nulls of Chebyshev's polynomials. In this study we have developed an efficient discrete mathematical model, performed a wide range of numerical experiments of wave diffraction on slits, and highlighted the efficiency and performance of applied DSM.



References

1. Gandel Yu.V., Dushkin V.D. Mathematical models of two-dimensional diffraction problems: Singular integral equations and numerical discrete singularities method (in Russian) / Monograph, Kharkov: Academy of Internal Defence of the MIA of Ukraine, 2012.
2. Gandel Yu.V. Boundary-Value Problems for the Helmholtz Equation and their Discrete Mathematical Models / Journal of Mathematical Sciences, Springer Science + Business Media Inc. 171 (1). – 2010. – P.74-88.
3. Gandel Yu.V., Kravchenko V.F., Pustovoit V.I. The scattering of electromagnetic waves by a thin superconducting strip (in Russian) // Proceedings of the Russian Academy of Sciences. – 1996. – 351;4. – P.462-464.
4. Gandel Yu.V., Dushkin V.D., Mathematical models based on SIE 2D diffraction problems on reflective multilayer periodic structures. Part I. The case of E-polarization (in Russian) // Belgorod State University Scientific Bulletin. Series: Mathematics. Physics. – 2011. – №5 (100). – P.5-16.
5. Gandel Yu.V., Nesvit K.V. Mathematical model of monochromatic wave diffraction problem on slits in the impedance plane which lies on the boundary of two media (in Russian) // Proceedings Russian Scientific-Technical Society of Radio Engineering, Electronics and Communication named after A.S. Popov, Moscow. – 2012. – №67. – P.114-117.
6. Nesvit K.V. Dirichlet boundary - value problem for the stationary wave equation, the boundary integral equation and its discrete mathematical models // Proceedings of the 2-nd International Scientific Conference of Students and Young Scientists "Theoretical and Applied Aspects of Cybernetics". Taras Shevchenko National University of Kyiv, Kyiv: Bukrek, 2012. – P.123-126.
7. Mandelbrot B.B. The Fractal Geometry of Nature / New York: W.H. Freeman and Company, 1983.
8. Akhiezer N.I. Lectures on Integral Transforms / Translations of Mathematical Monographs, American Mathematical Society. Providence, Rhode Island. 1988.
9. Gandel Yu.V. Introduction to methods of evaluation of singular and hypersingular integrals (in Russian) / Textbook. – Kharkov, Ukraine, 2002.
10. Watson G.N. A Treatise on the Theory of Bessel Functions / Cambridge At The University Press, 1922.
11. Colton D., Kress R. Integral equation methods in scattering / New York Chichester Brisbane. Toronto. Singapore: A Wiley Interscience Publication John Wiley & Sons, 1983.

**ГРАНИЧНЫЕ ИНТЕГРАЛЬНЫЕ УРАВНЕНИЯ
И ИХ ЧИСЛЕННЫЙ АНАЛИЗ В ЗАДАЧЕ ДИФРАКЦИИ
Е ПОЛЯРИЗОВАННОЙ ВОЛНЫ
НА ЩЕЛЯХ В ИМПЕДАНСНОЙ ПЛОСКОСТИ**

Ю.В. Гандель, Е.В. Несвит

Харьковский национальный университет им. В.Н. Каразина,
пл. Свободы, 4, Харьков, 61022, Украина, e-mail: yuriy.gandel@gmail.com, nesvit.k@gmail.com

Аннотация. В статье описывается подход к построению дискретной математической модели задачи дифракции E поляризованной волны на щелях в импедансной плоскости на базе



граничных интегральных уравнений (ИУ) соответствующей краевой задачи для стационарного волнового уравнения. Такие задачи приводят к системам граничных ИУ с логарифмическими особенностями в ядре, которые решаются эффективным методом дискретных особенностей (МДО). Показано, что дискретные математические модели задач дифракции волн на щелях и последующий численный эксперимент являются эффективным способом решения рассматриваемой задачи. В работе проведен численный анализ задачи дифракции E поляризованной волны на щелях и показаны основные характеристики электромагнитных полей при различных значениях параметров. Численные результаты приведены для диаграмм направленности и дифракционных картин рассеянного поля от предканторовых решеток различных порядков, а так же электрические и магнитные составляющие рассеянного электромагнитного поля в ближней зоне для различных значений импеданса решетки: Ag, Cu, Al, Mg, Ni и константана.

Ключевые слова: задача дифракции, граничные интегральные уравнения, численный анализ метода дискретных особенностей.